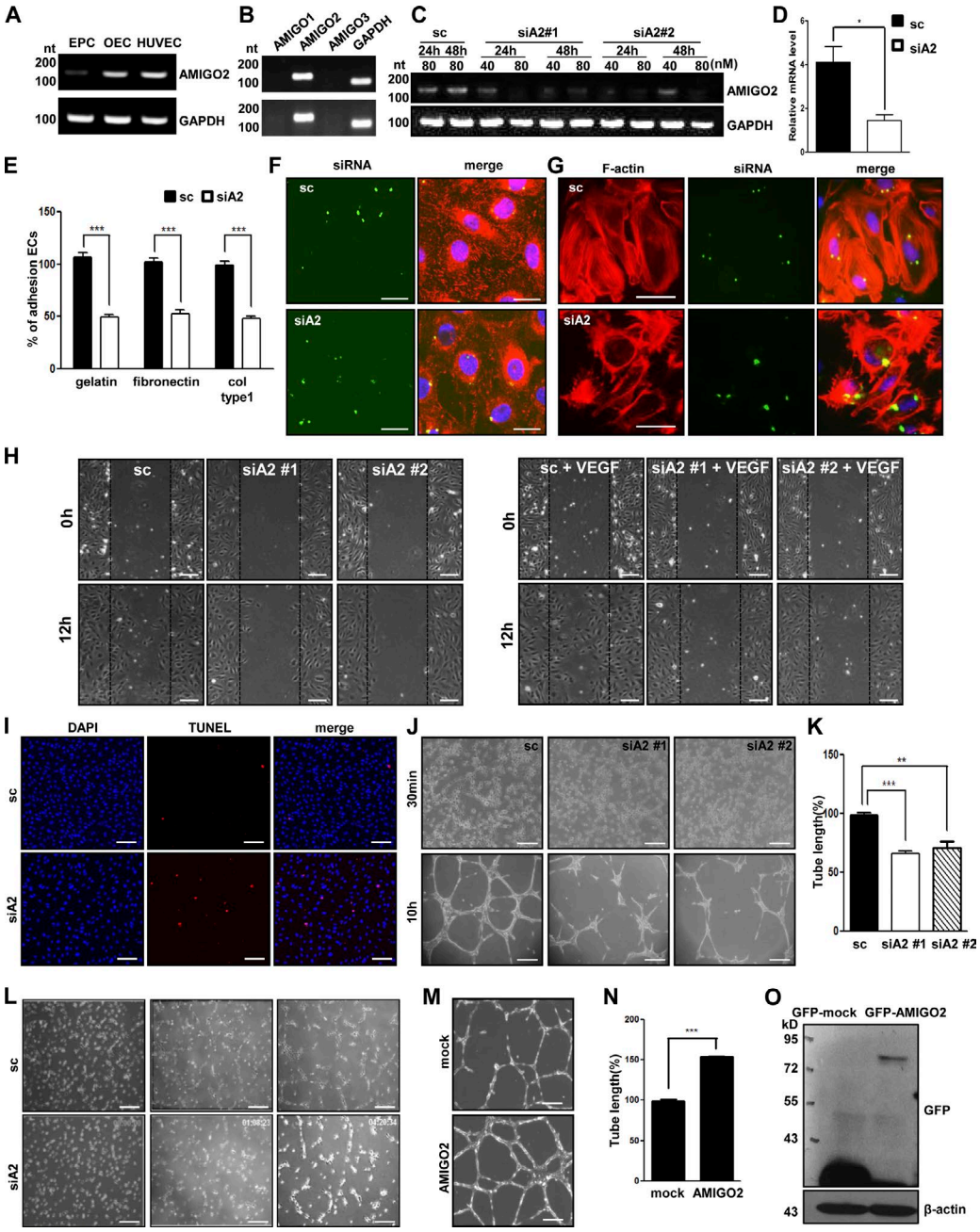

Figure S1. **AMIGO2 is specifically expressed in ECs and has angiogenic roles in ECs.** (A) AMIGO2 was highly expressed in differentiated ECs. Endothelial progenitor cells (EPC), outgrowth ECs (OEC), and HUVECs were examined. (B) The expression pattern of the AMIGO family was examined in two different types of HUVECs. (C) AMIGO2 mRNA levels in AMIGO2-depleted (siA2) and control (sc) ECs were measured in a time- and dose-dependent manner by RT-PCR. Two types of siA2 (siA2#1 and siA2#2) were evaluated. (D) AMIGO2 mRNA levels in AMIGO2-depleted (siA2#1; 48 h, 80 nM) and scrambled siRNA were measured by real-time PCR. (E–L) HUVECs were pretransfected with scrambled siRNA or siA2 before VEGF treatment. Cells were harvested for assay 48 h after transfection. (E) EC adhesion of AMIGO2-depleted HUVECs on gelatin-, fibronectin-, and collagen type 1–coated plates (n = 4). (F) FAK immunostaining was performed in parallel. FITC-siRNA and merged images of FAK and DAPI were captured. Bars, 20 µm. (G) Apoptotic cell shapes were detected by rhodamine-phalloidin staining for F-actin. Bars, 20 µm. (H) Wound healing migration with or without VEGF were performed. Two types of siA2 were evaluated for wound healing migration. Bar, 50 µm. (I) Visualization of TUNEL (red) and DAPI (blue) staining from AMIGO2 siRNA–transfected HUVECs. (J and K) Matrigel-induced tube-like structure formation was assessed. Two different types of siA2 were evaluated. Tube length is presented as the percentage of total tube length per field versus untreated control cells. n = 4. Bars, 200 µm. (L) Time-lapse captured images of Matrigel tube formation in AMIGO2 siRNA–transfected HUVECs. Bars, 200 µm. See Video 1. (M and N) Matrigel-induced tube formation by AMIGO2-overexpressed ECs was assessed. n = 3. Bars, 200 µm. (O) Overexpression of AMIGO2 in HUVECs was detected by Western blotting. *, $P < 0.05$; **, $P < 0.005$; ***, $P < 0.0001$. ns, not significant. Data are means ± SD.

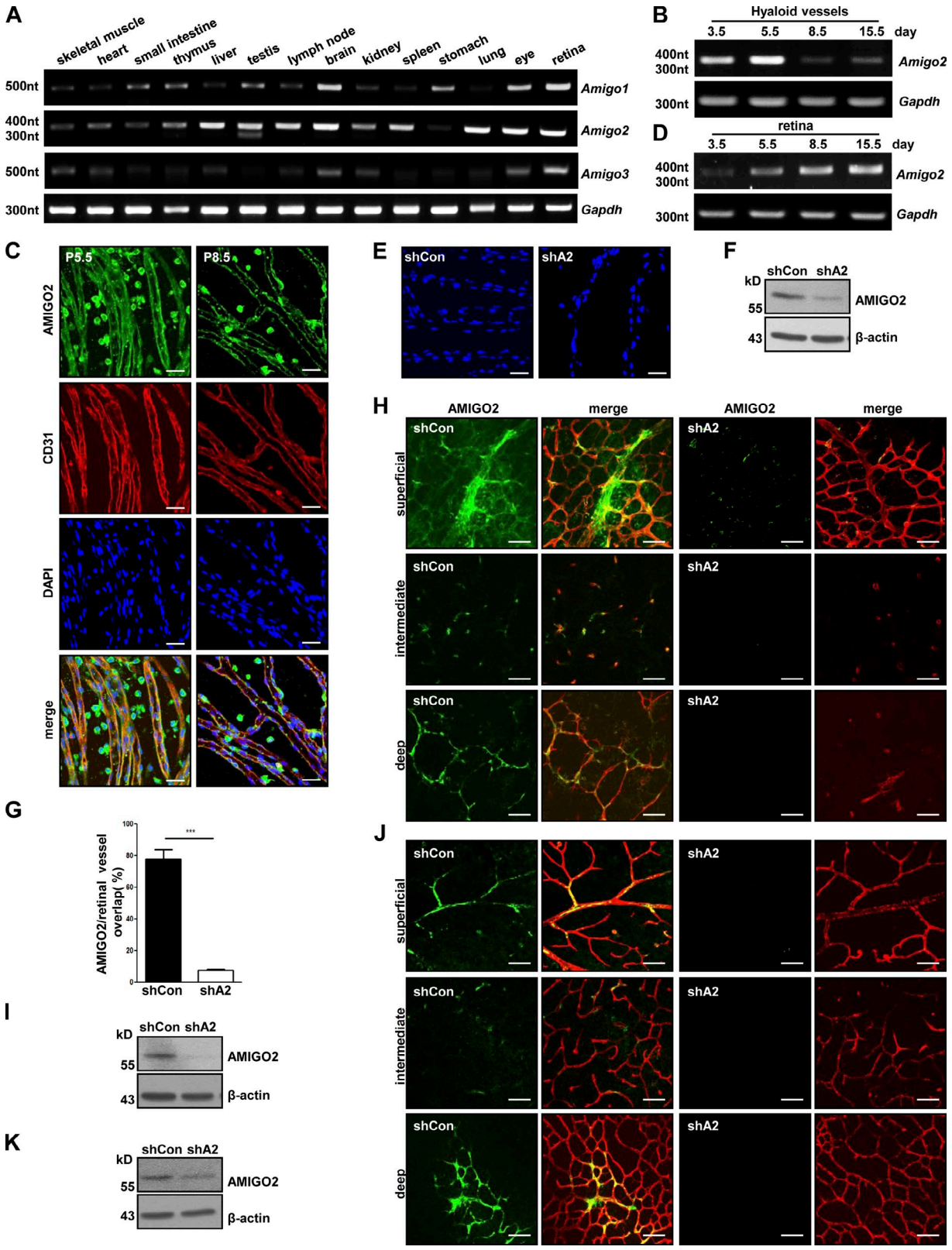

Figure S2. **AMIGO2 is expressed in hyaloid vessels and retinal vessels.** (A) AMIGO family expression pattern was verified in adult mouse tissues. (B and D) *Amigo2* expression level was measured in P3.5–15.5 mouse hyaloid vessels and retinas by RT-PCR. (C) Images show AMIGO2 in hyaloid vessels at P5.5 and 8.5. AMIGO2 (green), CD31 (EC marker; red), and DAPI (blue). (E) Hyaloid vessel staining with DAPI was performed in *Amigo2* shRNA–injected P5.5 mice. (F) AMIGO2 expression in *Amigo2* siRNA–injected mice at P5.5 was determined by Western blot analysis. (G) Quantification of the ratio of AMIGO2/iB4 in shCon- and *Amigo2* shRNA–injected mice at P5.5. (H and J) Immunostaining images of AMIGO2 (green), iB4 (red), and AMIGO2/iB4 merged color in retinal vessels at P8.5 (H) and at P15.5 (J). (I and K) Expression of AMIGO2 was evaluated in shCon- and *Amigo2* shRNA–injected mice at P8.5 (I) and at P15.5 (K) by Western blotting. Bars, 50 µm. ***, $P < 0.0001$. Data are means ± SD.

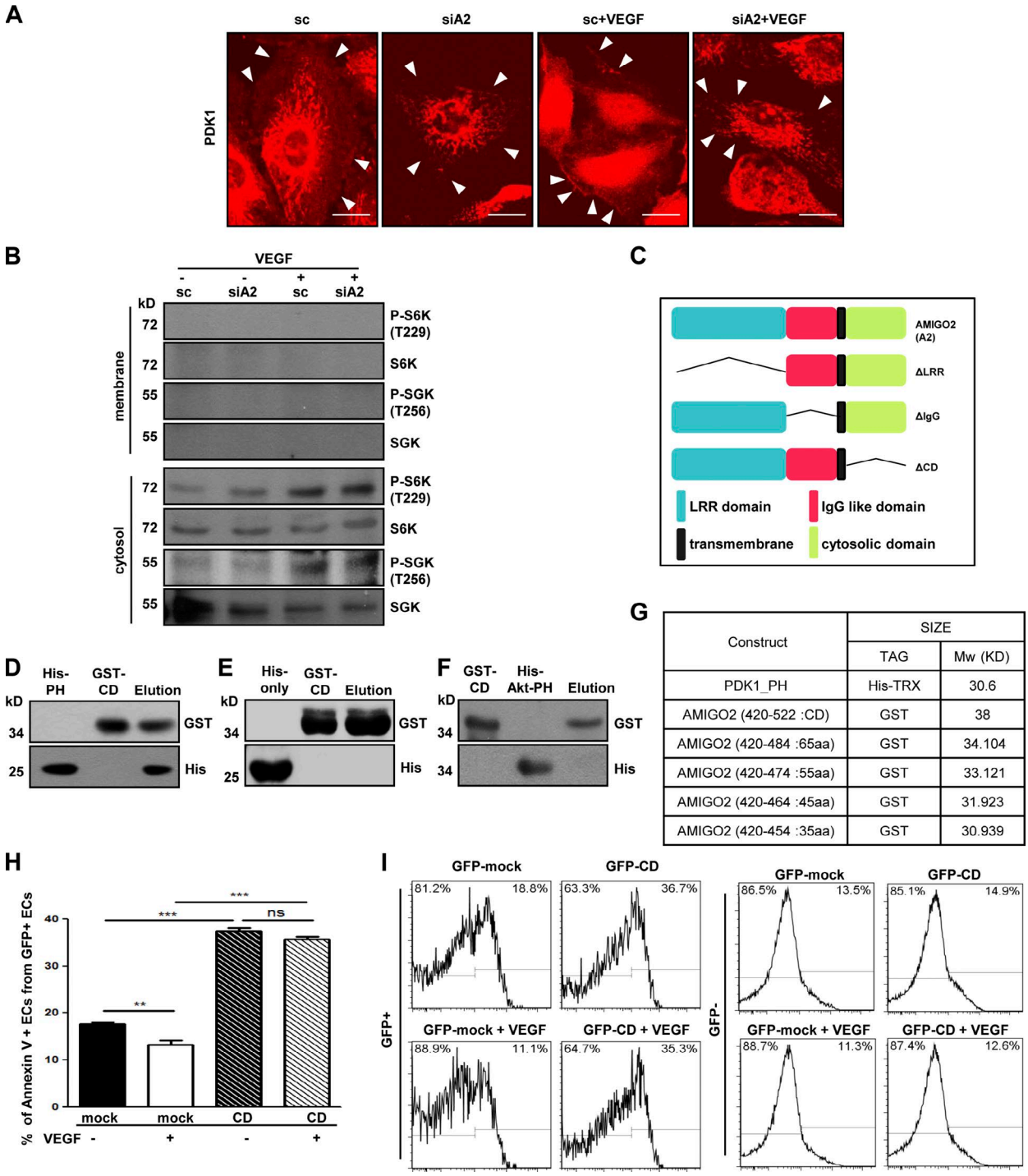

Figure S3. **The PH domain of PDK1 directly interacts with the CD of AMIGO2.** (A) PDK1 immunostaining was performed in AMIGO2-inhibited HUVECs in the presence or absence of VEGF. Images are enlarged from Fig. 4 A. Cells were starved for 6 h and treated with VEGF. White arrowheads point to membrane localization of PDK1. Bars, 20 μm. (B) Subcellular localization analysis was performed by cell fractionation in VEGF-treated, AMIGO2-deficient HUVECs. (C) Schematic diagrams of the wild type and three domain mutants of AMIGO2. $AMIGO2^{WT}$ refers to the wild type of AMIGO2, $AMIGO2^{\Delta LRR}$ refers to the LRR domain–deleted form of AMIGO2, $AMIGO2^{\Delta IgG}$ refers to the IgG domain–deleted form of AMIGO2, and $AMIGO2^{\Delta CD}$ refers to the CD domain–deleted form of AMIGO2. (D) His-tagged $PDK1^{PH}$ was incubated with purified GST-$AMIGO2^{CD}$. Mixtures of His- and GST-tagged proteins were pulled down with Ni^{2+}-NTA resin and analyzed by Western blotting using anti-GST and -His antibodies. (E) His-only protein was incubated with purified GST-$AMIGO2^{CD}$. Mixtures of His- and GST-tagged proteins were pulled down with Ni^{2+}-NTA resin and analyzed by Western blotting using anti-GST and -His antibodies. (F) His-tagged Akt PH domain was incubated with purified GST-$AMIGO2^{CD}$. Mixtures of His- and GST-tagged proteins were pulled down with GST resin and analyzed by Western blotting using anti-His and -GST antibodies. (G) A table of PH domain and AMIGO2 CD mutant protein sizes. (H) Quantification of flow cytometer analysis using annexin V staining. GFP-CD of AMIGO2-transfected HUVECs were cultured in serum-free starvation conditions with or without VEGF for 4 h (**, $P < 0.005$; ***, $P < 0.0001$; ns, not significant). Data were collected from four independent experiments and analyzed by a two-tailed unpaired *t* test. The values are means ± SD. (I) Flow cytometer analysis using annexin V staining. Values in plots indicate frequency (percentage) of parent. The data shown are from a single representative experiment out of four repeats (H).

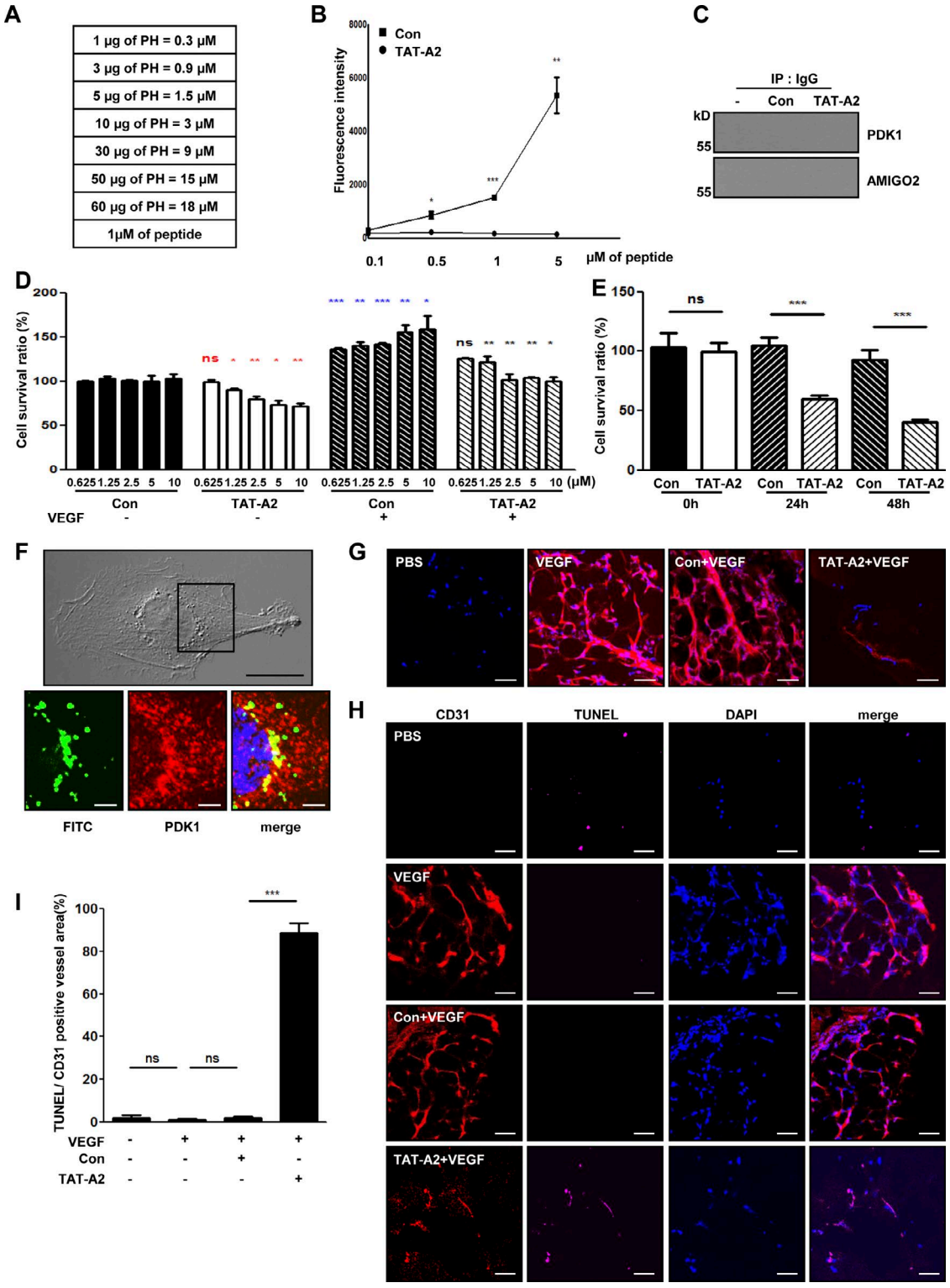

Figure S4. **PTD-A2 binds to the PH domain of PDK1 and inhibits AMIGO2 and PDK1 interaction.** (A) 0–60 μg PH domain proteins converted to micromole concentration. (B) 10 μg PH domain proteins were incubated with the CD domain of AMIGO2 and 0-, 0.1-, 0.5-, 1-, and 5-μM FITC-Con or TAT-A2 and detected by fluorescence. Data were collected from three independent experiments. (C) Con- and TAT-A2–treated HUVECs were immunoprecipitated with normal IgG antibody and blotted with anti-PDK1 and AMIGO2 antibodies. (D and E) Cell viability of TAT-A2–treated HUVECs under conditions of serum-free starvation with or without VEGF in a dose- and time-dependent manner. $n = 6$. (D) Comparison of cell survival rates between Con without VEGF and TAT-A2 without VEGF (red), between Con with and without VEGF (blue), and Con with VEGF and TAT-A2 with VEGF (black). (D and E) Data were collected from independent experiments and analyzed using a two-tailed unpaired *t* test. Data are means ± SD. (F) Colocalization of PDK1 and TAT-A2 in the HUVECs. (G) Merged images of Matrigel containing PBS, 200 ng VEGF, 25-μM Con with VEGF, or 25-μM TAT-A2 with VEGF. Immunolabeling with anti-CD31 antibody (red) and DAPI (blue) were used. Bars, 50 μm. (H) Immunolabeling with anti-CD31 antibody (red), TUNEL (pink), and DAPI (blue) was performed in Matrigel containing PBS, VEGF, Con with VEGF, or TAT-A2 with VEGF. Bars, 50 μm. (I) Quantification of TUNEL-positive areas over CD31-positive areas. *, $P < 0.05$; **, $P < 0.005$; ***, $P < 0.0001$. IP, immunoprecipitation; ns, not significant. Bars: (top) 20 μm; (bottom) 5 μm.

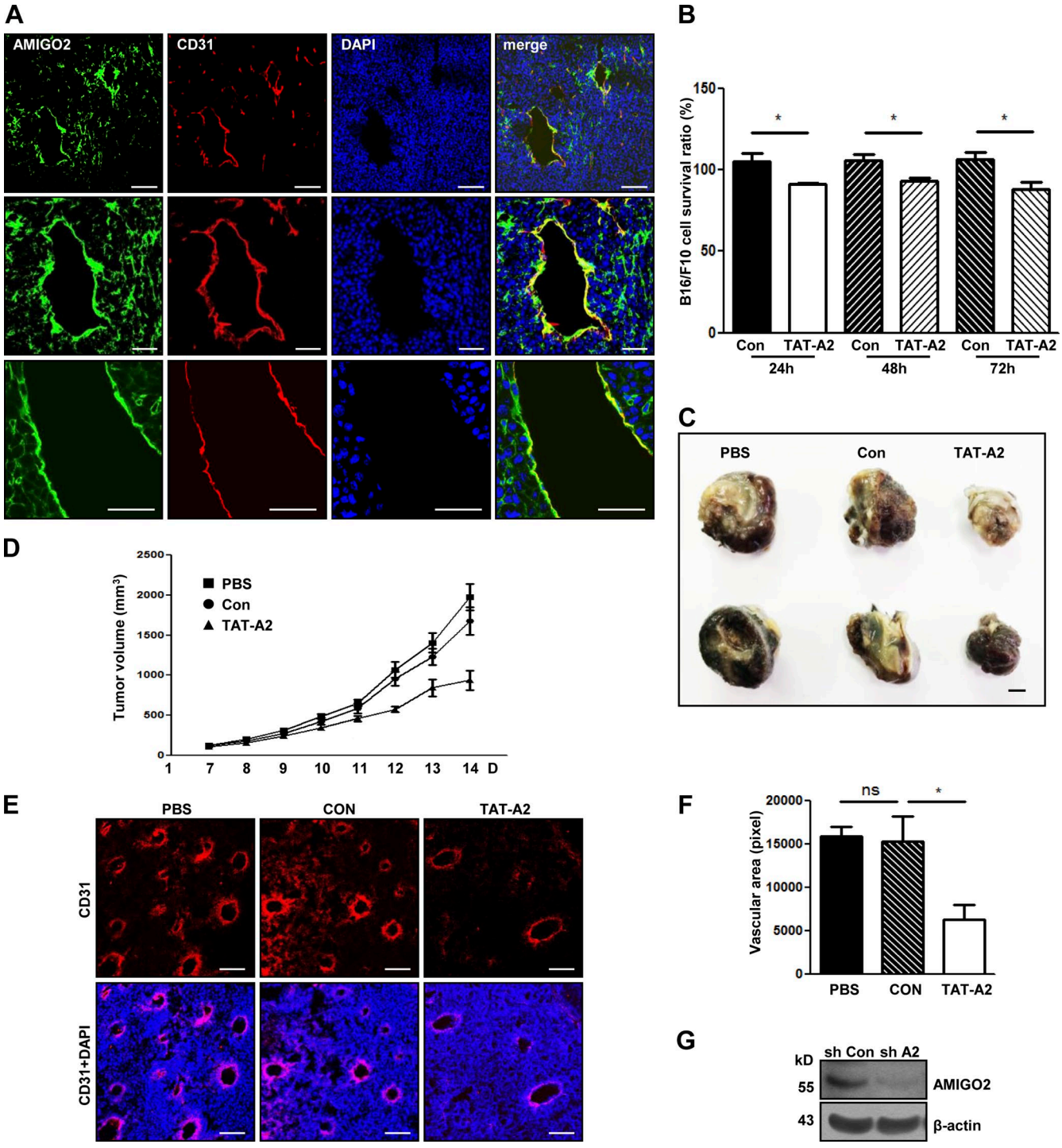

Figure S5. **PTD-A2 inhibits cell viability and tumorigenesis.** (A) Immunostaining of AMIGO2 (green), CD31 (red), and DAPI (blue) in B16F10 melanoma tumors. Bars: (top) 100 µm; (middle and bottom) 50 µm. (B) TAT-Con– or 5-µM A2-treated B16F10 cell viability by time. (C–F) Treatment with TAT-A2 inhibits tumor growth, neovessel formation, and tumor cell viability in B16F10 tumors. (C) Photograph of B16F10 melanoma tumors resected after 14 d. Bar, 5 mm. (D) Comparisons of tumor volume (n = 9 mice per group; 4 mg/kg Con or TAT-A2 was administered every other day). Data were analyzed using repeated measures of two-way analysis of variance. (E and F) Images (E) and quantification (F) of CD31-positive blood vessels (red) in B16F10 melanoma tumors. DAPI (blue). Bars, 100 µm. Data are means ± SD. (G) Expression of AMIGO2 was evaluated in shCon- and *Amigo2* shRNA–transfected B16F10 melanoma tumors by Western blotting. *, $P < 0.05$. ns, not significant.

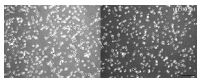

Video 1. **AMIGO2 siRNA–transfected ECs undergo anoikis in Matrigel tube formation.** HUVECs were transfected with AMIGO2 or scrambled siRNA and harvested at 24 h after transfection. AMIGO2- and scrambled siRNA–transfected HUVECs were seeded on Matrigel into a glass-bottomed dish. Matrigel tube formation in AMIGO2 siRNA–transfected HUVECs are on the right and control-transfected HUVECs are on the left. The video was taken with a digital camera (DP30BW; Olympus). This system was controlled and monitored in time-lapse mode by MetaMorph software (Molecular Devices). Frames were taken every 4 min for 7 h. Bar, 200 µm.